# Substituent Effect and Deuterium Isotope Effect of Ultrafast Intermolecular Electron Transfer: Coumarin in Electron-Donating Solvent

**Hideaki Shirota,[†,§] Haridas Pal,[‡,||] Keisuke Tominaga,[†,‡] and Keitaro Yoshihara*[,†,‡,⊥]**

*The Graduate University for Advanced Studies, Myodaiji, Okazaki 444, Japan, and Institute for Molecular Science, Myodaiji, Okazaki 444, Japan*

*Received: October 16, 1997; In Final Form: January 22, 1998*

Intermolecular electron transfer (ET), which occurs faster than solvation dynamics, has been investigated using the fluorescence up-conversion technique. The ultrafast ET processes have been observed from the electron-donating solvents to the excited coumarin dyes. In this work we have mainly focused our attention on the roles of the substitution of electron-donating solvent molecules in the ET dynamics. We have used aniline, *N*-monoalkylanilines, and *N*,*N*-dialkylanilines as electron-donating solvents and five 7-amino coumarins as acceptor molecules. For these systems the free energy gaps have been estimated from the cyclic voltammetry measurement and the steady-state absorption and fluorescence measurements. The experimental results indicate that the ET rate depends largely on the substituent groups of the solvent molecules. In *N*,*N*-dialkylanilines the ET rate gets smaller as the size of the alkyl substituent group becomes larger. For *N*-monoalkylanilines, however, the ET dynamics are not changed by the different alkyl substituent groups. In many donor−acceptor combinations we recognized that the ET rate is much faster than the solvation time. We simulated the results by the two-dimensional ET model with solvent and nuclear coordinates and found that the *N*-alkyl substituent effect on the ET rate appears to be mainly due to the changes in the electronic matrix element. We have also investigated the deuterium isotope effect on the ET dynamics using *N*-deuterated-*N*-monoalkylanilines as donor solvents. For the fastest ET the isotope effect is hardly observable, whereas the effect is quite large (∼20%) for slower ET. The deuterium isotope effect seems to mainly come from the change of stabilization energies in intermolecular hydrogen-bonding interaction by deuteration. The extent of deuterium isotope effect on ET is similar for all *N*-monoalkylanilines used. This result indicates that the size of the alkyl groups does not affect much the hydrogen-bonding interaction.

## 1. Introduction

Electron transfer (ET) plays a key role in chemical reactions, photography, solar cell, biosynthesis, photosynthesis, and other processes. Because of the fundamental nature of the ET dynamics, many scientists and engineers have paid great attentions to investigate the different aspects of the ET phenomena.[1−17] Similar to other chemical reactions, ET is a phenomenon of free energy surface crossing from the reactant state to the product state. In the transition-state theory, the reaction rate constant ($k_{TST}$) can be written as

$$k_{TST} = \frac{P\omega_0}{2\pi} \exp\left(-\frac{\Delta G^*}{k_B T}\right) \tag{1}$$

where $P$ is the electronic-transition probability at the transition region, $\omega_0$ is the frequency of motion in the reactant potential well, and $\Delta G^*$ is the free energy of activation. ET in liquid state is a phenomenon which suddenly changes the charge distribution; thus, one must consider an effect of the stabilization energy of solvent molecules around the solutes (reorganization energy) following the ET process. The reorganization of the solvent molecules had often been treated as fast enough compared to the ET.

In the case of ET, the probability $P$ can be determined by the electronic matrix element $V_{el}$, which is approximately proportional to an overlap integral between the wave functions of the reactant and product states. In the nonadiabatic limit where $V_{el}$ is very small, the rate constant of ET ($k_{NA}$) can be written as[18,19]

$$k_{NA} = \frac{2\pi}{\hbar} \frac{V_{el}^2}{\sqrt{4\pi\lambda_s k_B T}} \exp\left(-\frac{\Delta G^*}{k_B T}\right) \tag{2}$$

where $\lambda_s$ is the solvent reorganization energy. According to the Marcus theory,[19] $\Delta G^*$ is expressed as

$$\Delta G^* = \frac{(\lambda_s + \Delta G^0)^2}{4\lambda_s} \tag{3}$$

where $\Delta G^0$ is the free energy gap between the product and reactant states.

In the adiabatic ET, $P$ in eq 1 becomes unity. The frequency of the motion $\omega_0$ is determined by the solvent fluctuation, and the quasi-particle crosses the transition state by Brownian motion.[20] When the adiabaticity parameter $\kappa$ is included in ET,

† The Graduate University for Advanced Studies.
‡ Institute for Molecular Science.
§ Present address: Department of Chemistry and Biotechnology, Graduate School of Engineering, The University of Tokyo, 7-3-1 Hongo, Bunkyo-ku, Tokyo 113, Japan.
|| Present address: Chemistry Division, Bhabha Atomic Research Centre, Bombay 400 085, India.
⊥ Present address: Japan Advanced Institute of Science and Technology, Hokuriku, Tatsunokuchi 923-12, Japan.

S1089-5639(97)03376-8 CCC: $15.00 
Published on Web 04/15/1998

the rate constant is given by[20−22]

$$k_{ET} = k_{NA}/(1+\kappa) \tag{4}$$

$$\kappa = \frac{4\pi V_{el}^2 \tau_s}{\hbar \lambda_s} \tag{5}$$

where $\tau_s$ is the solvation time. The uniqueness of eq 4 is that it describes ET from the nonadiabatic limit ($\kappa \ll 1$) to the adiabatic limit ($\kappa \gg 1$) in one expression. In the adiabatic limit, the rate constant ($k_A$) can be written as[22,23]

$$k_A = \frac{1}{\tau_s}\sqrt{\frac{\lambda_s}{16\pi k_B T}} \exp\left(-\frac{\Delta G^*}{k_B T}\right) \tag{6}$$

The value of $16\pi k_B T$ at room temperature is about 1.3 eV. Since the value of $\lambda_s$ is normally either close to or less than this value, eq 6 indicates that the maximum ET rate constant (barrierless reaction) should be equal to $\tau_s^{-1}$. For ultrafast ET occurring in the picosecond time scale or slower, it is thus expected that the solvent fluctuations will be the rate determining factor.

Recently, we have reported[14,24−32] a new type ET which occurs much faster than the solvation dynamics. This ultrafast intermolecular ET occurs from the electron donating solvents (aniline (AN) and *N*,*N*-dimethylaniline (DMA)) to the excited ($S_1$) dyes (oxazine-1, Nile blue, and coumarins). To investigate the mechanism, we have studied the substituent effect of the acceptor molecule on ET and the isotope effect on ET in the coumarin−aniline system. To explain the ultrafast nature of these ET dynamics, we consider both intramolecular vibrational motions and intermolecular motions in a different fashion to describe the ET process (two-dimensional (2D) coordinate ET model[33−36]). With the 2D-ET model, the aspects of the ultrafast ET dynamics have quite successfully been explained.[14,31,32,37−39] On the basis of the research of the substituent effect of the coumarin dye, the ET rate dependence on the substituent group was determined mainly come from the reduction potential of the coumarin dye.[27,31] The result of the isotope effects on the ET have shown that the isotope effect appears in only AN and mostly arises from the difference of $\Delta G^0$ due to the change of stabilization energy of the hydrogen-bonding interaction.[32]

In this work we investigate the substituent effect and deuterium isotope effect of electron donating solvent on the ET dynamics to study the reaction mechanism further. We focus our attention on a couple of specific problems on ET.

**(i) Solvent Effect.** So far, only two solvents (AN and DMA) was investigated, and the difference of the ET dynamics in AN and DMA was concluded to mainly arises from the different $\Delta G^0$ values. Using other related aniline derivatives as solvent, we can study the roles of the natures of the electron donor and solvent in the ET reaction

**(ii) Estimation of $\Delta G^0$.** A reliable estimation of $\Delta G^0$ is required for a quantitative discussion on ET dynamics. However, it is quite difficult to obtain accurate values of $\Delta G^0$ experimentally for the ET in the excited state in less polar solvents. We estimate the $\Delta G^0$ values in an empirical fashion for all the systems investigated

**(iii) Solvent Isotope Effect.** We observed the solvent isotope effect on the ET dynamics in the case of AN and interpreted it due to the change of the hydrogen-bonding interaction. It is interesting to see the solvent isotope effect for other related hydrogen-bonding solvents.

This paper is organized in the following way. The experimental methods are mentioned in section 2. Section 3 presents the experimental results of substituent effect and deuterium isotope effect on ET rates, solvation, and redox potentials of dyes and solvents. Section 4 explains the estimation of the $\Delta G^0$ for the present systems. 2D-ET model and ET parameters for simulation are mentioned in section 5. The results of experiments and simulations are discussed in section 6, followed by a brief summary in section 7.

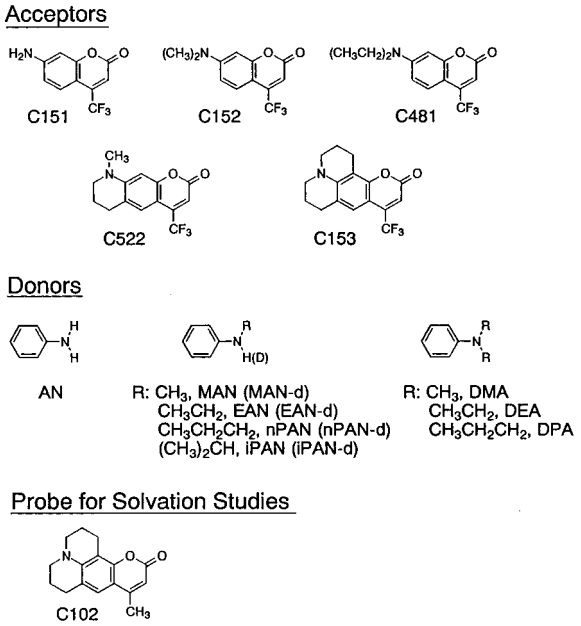


**Figure 1.** The structures of the molecules used in this experiment. Abbreviations of the names of the molecules are also given.

## 2. Experimental Section

**2.1. Sample Preparation.** The molecular structures of the dye molecules and the normal and deuterated solvents used in the present work are shown in Figure 1. Laser grade coumarin dyes (C151, C152, C481, C522, C153, or C102) were purchased from Exciton, Lambda Physik, and Eastman Kodak and used without further purification. Aniline (AN), *N*-monoalkylanilines (*N*-methylaniline; MAN, *N*-ethylaniline; EAN, *N*-propylaniline; nPAN, and *N*-isopropylaniline; iPAN), and *N*,*N*-dialkylanilines (*N*,*N*-dimethylaniline; DMA, *N*,*N*-diethylaniline; DEA, and *N*,*N*-dipropylaniline; DPA) were obtained from Tokyo Kasei and used after vacuum distillation. Deuterated *N*-monoalkylanilines (*N*-deuterio-*N*-methylaniline; MAN-*d*, *N*-deuterio-*N*-ethylaniline; EAN-*d*, *N*-deuterio-*N*-propylaniline; nPAN-*d*, and *N*-deuterio-*N*-isopropylaniline; iPAN-*d*) were prepared from the normal solvents by isotope exchange reaction with $D_2O$ and were purified by vacuum distillation. The isotopic purity of each deuterated *N*-monoalkylaniline was estimated to be more than 90% by IR measurement.

**2.2. Femtosecond Fluorescence Up-Conversion Measurement.** Details of the fluorescence up-conversion apparatus were reported elsewhere.[24,30−32] Briefly, the fundamental of a femtosecond titanium:sapphire laser (Spectra Physics, Tsunami) at around 800 nm with an average power of about 550 mW was used to produce the second harmonic at 400 nm with an average power of about 50 mW in a 1 mm BBO crystal (type I). The second harmonic was used to excite the sample and the remaining fundamental was used as the probe beam to up-convert the fluorescence from the sample in a 0.3 mm BBO crystal (type I). The cross-correlation measured between the second harmonic and the fundamental had a full width at half-maximum of 210 fs. The angle between the polarization of

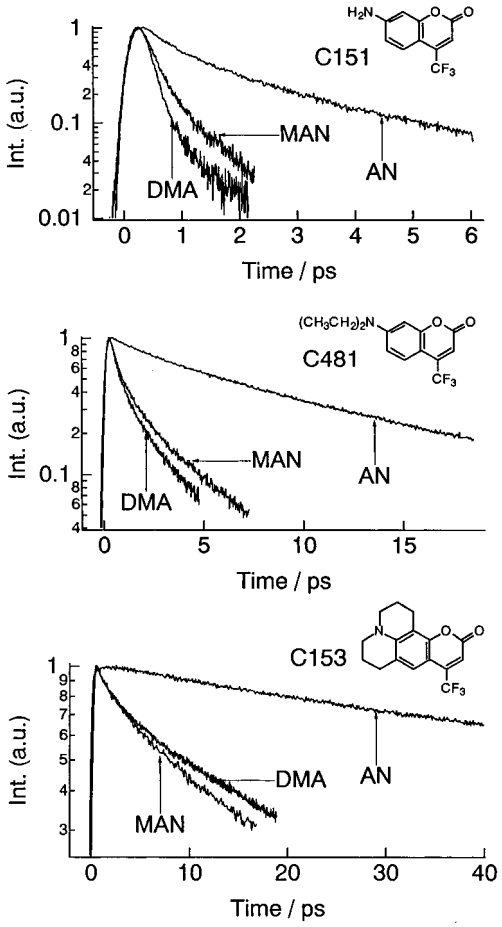


**Figure 2.** Fluorescence decays of C151 (top), C481, and C153 (bottom) in AN, MAN, and DMA, excited at 400 nm and observed at the peaks of the steady-state fluorescence spectra.

pump and probe beams was adjusted to the magic angle by a half-wave plate. The up-converted signal was detected with a photon-counting system after passing through a monochromator. The concentrations of dyes were around $10^{-3}$ M. The optical path length of the sample was 1 mm. The samples were circulated during measurements, and all the measurements were made at 294 K.

**2.3. Cyclic Voltammetric Measurement.** Cyclic voltammetric measurements (Bioanalytical Systems, Inc., Model BAS100B) were carried out using Pt working, Pt wire auxiliary, and SCE reference electrodes. As the supporting electrolyte, tetrabutylammonium perchlorate (polarography grade, Nacalai Tesque) was used and the concentration was kept at 0.1 M. The solute concentrations were $4 \times 10^{-3}$ M for the reduction-potential measurement of the coumarin dyes in acetonitrile and 0.01 M for the oxidation-potential measurement of normal and deuterated aniline, *N*-monoalkylanilines, and *N*,*N*-dialkylanilines in methanol, deuterated methanol ($CH_3OD$), and acetonitrile. The redox potentials were determined at the peak positions of CV curve because the compounds showed the irreversible feature.

## 3. Results

**3.1. Substituent Effect of Electron-Donating Solvent on Electron-Transfer Dynamics.** *3.1.1. Aniline, N-Methylaniline, and N,N-Dimethylaniline.* Figure 2 compares the fluorescence decays obtained for the several coumarin dyes (C151 (fastest fluorescence decay system), C481, and C153 (slowest fluorescence decay system)) in aniline (AN), *N*-methylaniline (MAN), and *N*,*N*-dimethylaniline (DMA) measured near the peaks of the steady-state fluorescence spectra of the coumarin dyes. It is evident from this figure that for all cases the fluorescence decays are nonsingle exponential. All the decay curves are tentatively analyzed with a biexponential function ($a_1 \exp(-t/\tau_1) + a_2 \exp(-t/\tau_2)$; $a_1 + a_2 = 1$) convoluting the instrument response by the global unlimited fitting program. The fitting curve for the decay of C151 in MAN is shown in Figure 3 as a typical example. The cross-correlation between the second harmonic and fundamental of the titanium:sapphire laser pulse. All of the curves are well fitted by a biexponential function. Table 1 lists the fluorescence lifetimes analyzed and the average lifetimes ($\langle\tau\rangle$) calculated as,

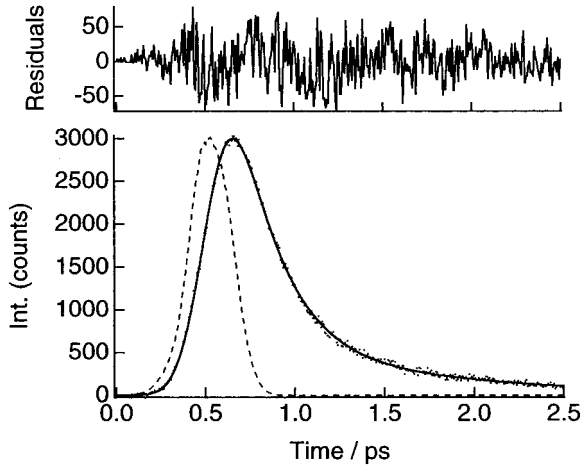


**Figure 3.** Fluorescence decays of C151 in MAN excited at 400 nm and observed at the peak wavelength of the steady-state fluorescence spectra (440 nm) (dots). The decay curve is nonexponential, and this is analyzed by a biexponential fitting curve (line). Broken line shows the cross-correlation measured between the second harmonic and the fundamental of a titanium:sapphire laser $\chi^2$ is 1.8.

$$\langle\tau\rangle = a_1\tau_1 + a_2\tau_2 \tag{7}$$

The tendency of the fluorescence lifetimes of each coumarin dyes are similar ($\langle\tau\rangle$(AN) $\gg$ $\langle\tau\rangle$(MAN) > $\langle\tau\rangle$(DMA)) except for C153. The trend of the change of the fluorescence lifetime of coumarin is the same for all the solvent examined, AN, MAN, and DMA, namely, $\langle\tau\rangle$(C153) > $\langle\tau\rangle$(C522) > $\langle\tau\rangle$(C481) > $\langle\tau\rangle$(C152) > $\langle\tau\rangle$(C151).

In solvents such as methanol or hexane the fluorescence lifetimes of coumarins are several nanoseconds.[40−42] However, the fluorescence lifetimes of some coumarins are drastically reduced in electron donating solvents such as AN and DMA.[27−32] We ascribed this drastic reduction to intermolecular ET from the electron donating solvents to the excited ($S_1$) coumarins. These reactions are similar to those of Nile blue and oxazine-1 in AN and DMA.[24−26,28−30] In the latter cases the products (the radical cations of solvents and the neutral radicals of dyes) were observed by the subpicosecond transient absorption measurement.[25,29]

*3.1.2. N-Monoalkylanilines.* Figure 4 shows the fluorescence decays of C151 and C153 in a series of *N*-monoalkylanilines, i.e., in MAN, *N*-ethylaniline (EAN), *N*-propylaniline (nPAN), and *N*-isopropylaniline (iPAN). For both the cases of C151 and C153 the fluorescence decays are highly nonsingle exponential. An interesting point is that for each coumarin the fluorescence decays in all *N*-monoalkylanilines are rather

**TABLE 1: Fluorescence Lifetimes of Coumarins in AN, Normal and *N*-Deuterated *N*-Monoalkylnilines, and *N,N*-Dilakylnilines**

| acceptor | donor | $a_1$ | $\tau_1$/ps | $a_2$ | $\tau_2$/ps | $\langle\tau\rangle^a$/ps | $\langle\tau\rangle_d/\langle\tau\rangle_h$ |
|---|---|---|---|---|---|---|---|
| C151 | AN | 0.63 | 0.66 | 0.37 | 3.15 | 1.58 | |
| | MAN | 0.88 | 0.25 | 0.12 | 1.09 | 0.35 | |
| | MAN-*d* | 0.92 | 0.30 | 0.08 | 1.11 | 0.36 | 1.03 |
| | EAN | 0.86 | 0.25 | 0.14 | 1.18 | 0.38 | |
| | EAN-*d* | 0.82 | 0.21 | 0.18 | 1.25 | 0.40 | 1.05 |
| | nPAN | 0.82 | 0.22 | 0.18 | 1.34 | 0.42 | |
| | nPAN-*d* | 0.80 | 0.20 | 0.20 | 1.26 | 0.41 | 0.98 |
| | iPAN | 0.83 | 0.30 | 0.17 | 1.38 | 0.48 | |
| | iPAN-*d* | 0.80 | 0.24 | 0.20 | 1.34 | 0.46 | 0.96 |
| | DMA | 0.96 | 0.20 | 0.04 | 0.60 | 0.22 | |
| | DEA | 0.90 | 0.23 | 0.10 | 1.02 | 0.31 | |
| | DPA | 0.81 | 0.24 | 0.19 | 2.19 | 0.61 | |
| C152 | AN | 0.41 | 2.35 | 0.59 | 10.7 | 7.3 | |
| | MAN | 0.71 | 0.45 | 0.29 | 2.64 | 1.09 | |
| | MAN-*d* | 0.74 | 0.53 | 0.26 | 3.15 | 1.21 | 1.11 |
| | EAN | 0.72 | 0.43 | 0.28 | 3.10 | 1.18 | |
| | EAN-*d* | 0.73 | 0.47 | 0.27 | 3.58 | 1.31 | 1.11 |
| | nPAN | 0.73 | 0.46 | 0.27 | 3.74 | 1.35 | |
| | nPAN-*d* | 0.71 | 0.49 | 0.29 | 3.86 | 1.47 | 1.09 |
| | iPAN | 0.70 | 0.47 | 0.30 | 4.05 | 1.54 | |
| | iPAN-*d* | 0.68 | 0.48 | 0.32 | 4.13 | 1.65 | 1.07 |
| | DMA | 0.82 | 0.41 | 0.18 | 2.44 | 0.78 | |
| | DEA | 0.78 | 0.38 | 0.22 | 2.54 | 0.86 | |
| | DPA | 0.72 | 0.38 | 0.28 | 3.83 | 1.35 | |
| C481 | AN | 0.37 | 3.5 | 0.63 | 14.2 | 10.2 | |
| | MAN | 0.69 | 0.52 | 0.31 | 3.35 | 1.40 | |
| | MAN-*d* | 0.69 | 0.61 | 0.31 | 3.85 | 1.61 | 1.15 |
| | EAN | 0.68 | 0.50 | 0.32 | 3.80 | 1.56 | |
| | EAN-*d* | 0.66 | 0.55 | 0.34 | 4.17 | 1.78 | 1.14 |
| | nPAN | 0.68 | 0.53 | 0.32 | 4.25 | 1.72 | |
| | nPAN-*d* | 0.65 | 0.53 | 0.35 | 4.55 | 1.94 | 1.13 |
| | iPAN | 0.67 | 0.62 | 0.33 | 5.35 | 2.18 | |
| | iPAN-*d* | 0.64 | 0.68 | 0.36 | 5.59 | 2.45 | 1.12 |
| | DMA | 0.68 | 0.40 | 0.32 | 2.30 | 1.01 | |
| | DEA | 0.70 | 0.60 | 0.30 | 4.23 | 1.69 | |
| | DPA | 0.64 | 0.52 | 0.36 | 5.19 | 2.20 | |
| C522 | AN | 0.31 | 8.9 | 0.69 | 33.6 | 25.9 | |
| | MAN | 0.55 | 1.38 | 0.45 | 8.17 | 4.44 | |
| | MAN-*d* | 0.55 | 1.70 | 0.45 | 9.63 | 5.27 | 1.19 |
| | EAN | 0.56 | 1.41 | 0.44 | 9.49 | 4.97 | |
| | EAN-*d* | 0.52 | 1.54 | 0.48 | 10.8 | 5.98 | 1.20 |
| | nPAN | 0.59 | 1.24 | 0.41 | 10.4 | 5.00 | |
| | nPAN-*d* | 0.54 | 1.44 | 0.46 | 11.3 | 5.98 | 1.20 |
| | iPAN | 0.56 | 1.47 | 0.44 | 11.6 | 5.93 | |
| | iPAN-*d* | 0.53 | 1.63 | 0.47 | 13.2 | 7.07 | 1.19 |
| | DMA | 0.69 | 0.80 | 0.31 | 4.00 | 1.79 | |
| | DEA | 0.52 | 0.96 | 0.48 | 8.97 | 4.80 | |
| | DPA | 0.52 | 0.84 | 0.48 | 12.9 | 6.63 | |
| C153 | AN | 0.38 | 15.2 | 0.62 | 118.0 | 79.0 | |
| | MAN | 0.40 | 3.0 | 0.60 | 22.8 | 14.9 | |
| | MAN-*d* | 0.35 | 4.7 | 0.65 | 25.4 | 18.2 | 1.22 |
| | EAN | 0.42 | 3.5 | 0.58 | 25.5 | 16.3 | |
| | EAN-*d* | 0.40 | 4.0 | 0.60 | 29.5 | 19.3 | 1.20 |
| | nPAN | 0.47 | 3.3 | 0.53 | 25.1 | 14.9 | |
| | nPAN-*d* | 0.42 | 3.5 | 0.58 | 28.3 | 17.9 | 1.20 |
| | iPAN | 0.43 | 3.0 | 0.57 | 26.8 | 16.6 | |
| | iPAN-*d* | 0.43 | 3.7 | 0.57 | 32.4 | 20.1 | 1.21 |
| | DMA | 0.30 | 3.4 | 0.70 | 25.1 | 18.6 | |
| | DEA | 0.27 | 4.0 | 0.73 | 54.4 | 40.8 | |
| | DPA | 0.24 | 3.8 | 0.76 | 70.3 | 54.3 | |

[a] $\langle\tau\rangle = a_1\tau_1 + a_2\tau_2$; $a_1 + a_2 = 1$.

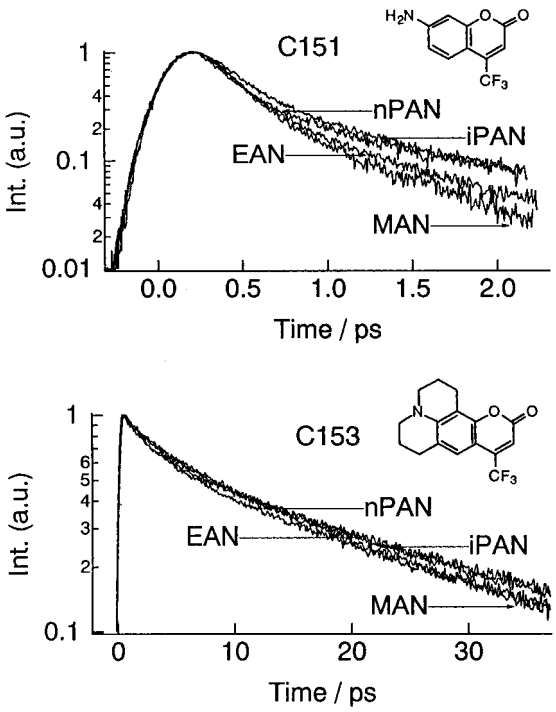


**Figure 4.** Fluorescence decays of C151 (top) and C153 (bottom) in *N*-monoalkylanilines, namely, MAN, EAN, nPAN, and iPAN. Excited wavelength is 400 nm, and observed wavelength are the peaks of the steady-state fluorescence spectra.

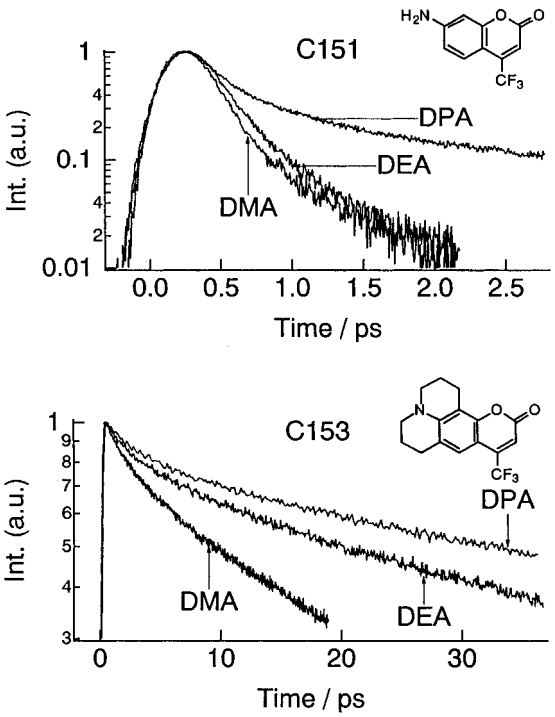


**Figure 5.** Fluorescence decays of C151 (top) and C153 (bottom) in *N,N*-dialkylanilines, namely, DMA, DEA, DPA. Excited wavelength is 400 nm, and observed wavelength are the peaks of the steady-state fluorescence spectra.

similar. The same feature is also observed in all the other coumarins (C152, C481, and C522). All the fluorescence decays are analyzed by the same procedure and the parameters obtained are summarized in Table 1.

*3.1.3. N,N-Dialkylanilines.* Figure 5 shows the fluorescence decays of C151 and C153 in *N,N*-dialkylaniline, namely, in DMA, *N,N*-diethylaniline (DEA), and *N,N*-dipropylaniline (DPA). It is clear that the fluorescence decays are also nonsingle exponential in both the cases of the fastest ET (C151) and slowest ET (C153). The other dyes (C152, C481, and C522) show also a nonsingle-exponential feature.

In *N,N*-dialkylanilines the fluorescence decays are dependent on the solvents drastically: $\langle\tau\rangle$(DPA) > $\langle\tau\rangle$(DEA) > $\langle\tau\rangle$(DMA). This is in contrast to the cases of *N*-monoalkylaniline. This

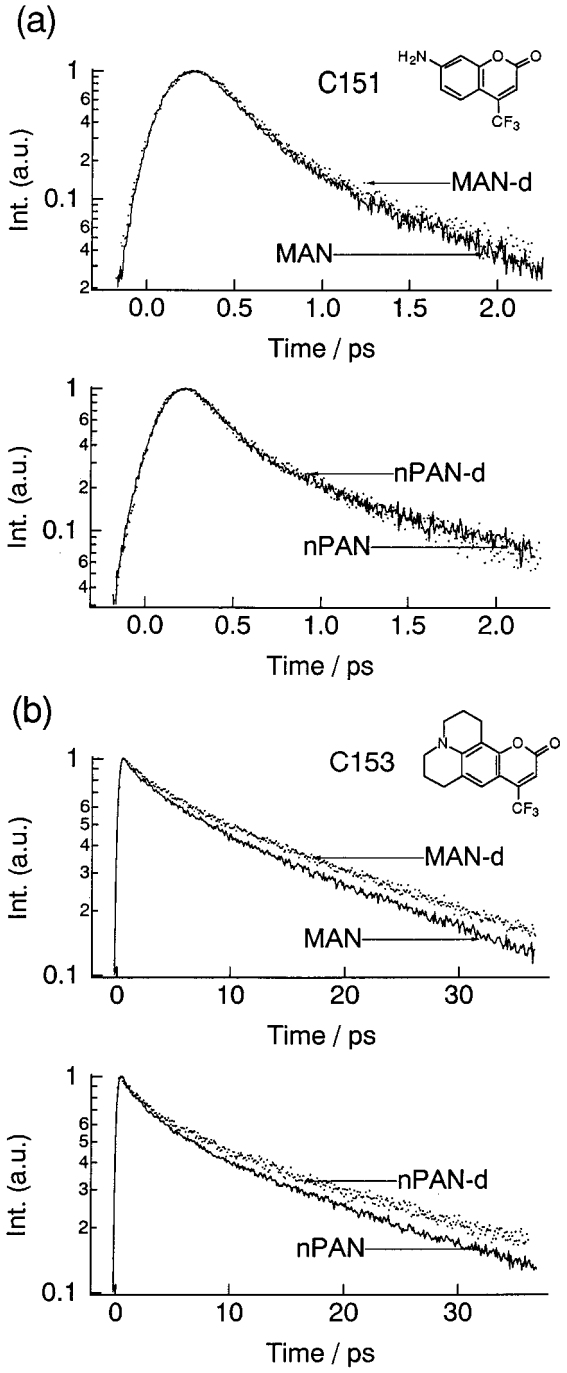


**Figure 6.** Comparison of the fluorescence decays of coumarins in MAN (solid lines), MAN-*d* (dotted lines), nPAN (solid lines), and nPAN-*d* (dotted lines): (a) C151 and (b) C153. The deuterium isotope effect on the slow dye (C153) is very clear, but no deuterium isotope effect on the fast dye (C151).

trend is also observed in the other coumarins (C152, C481, and C522). The fluorescence decay parameters analyzed are listed in Table 1.

**3.2. Deuterium Isotope Effect on the Electron-Transfer Dynamics: N-Monoalkylanilines.** Figure 6 compares the fluorescence decays of C151 and C153 in normal and deuterated *N*-monoalkylanilines (MAN and MAN-*d*, and nPAN and nPAN-*d*) observed at the vicinity of the peaks of the steady-state fluorescence spectra of the dyes. The absorption and fluorescence spectra of the coumarin dyes in normal and deuterated *N*-monoalkylanilines are identical to the case of aniline.[32] The important point to be noted is the fluorescence decays become slower in deuterated *N*-monoalkylanilines than those in normal *N*-monoalkylanilines in the case of C153 (slowest fluorescence decay system). In the case of C151 (fastest fluorescence decay system), however, the fluorescence decays in the deuterated solvents are almost similar to those in the normal solvents (Table 1). For the other coumarins (C152, C481, and C522) the fluorescence decays in the deuterated solvents become also slower than in the normal solvents (Table 1). Table 1 also lists the isotope effect on $\langle\tau\rangle$, namely $\langle\tau\rangle_d/\langle\tau\rangle_h$. Here $\langle\tau\rangle_d$ and $\langle\tau\rangle_h$ are the average lifetimes in the deuterated and normal solvents, respectively. It is clear from Table 1 that the slower fluorescence decay systems show a greater isotope effect on $\langle\tau\rangle$. The extent of the isotope effect in each coumarin is seen to be almost the same for all the *N*-monoalkylanilines.

**TABLE 2: Solvation Parameters for AN, Normal and *N*-Deuterated *N*-Monoalkylnilines, and *N*,*N*-Dilakylnilines**

| solvent | $a_{s1}$ | $\tau_{s1}$/ps | $a_{s2}$ | $\tau_{s2}$/ps | $\langle\tau_s\rangle^a$/ps | $\langle\tau_s\rangle_d/\langle\tau_s\rangle_h$ |
|---|---|---|---|---|---|---|
| AN | 0.28 | 1.2 | 0.72 | 17.8 | 13.2 | |
| MAN | 0.25 | 2.0 | 0.75 | 16.2 | 12.2 | |
| MAN-*d* | 0.24 | 2.5 | 0.76 | 18.5 | 14.7 | 1.20 |
| EAN | 0.24 | 2.0 | 0.76 | 19.1 | 15.0 | |
| EAN-*d* | 0.23 | 2.9 | 0.77 | 22.8 | 18.2 | 1.21 |
| nPAN | 0.21 | 2.2 | 0.79 | 19.3 | 15.7 | |
| nPAN-*d* | 0.23 | 3.0 | 0.77 | 24.1 | 19.2 | 1.22 |
| iPAN | 0.23 | 2.3 | 0.77 | 20.3 | 16.2 | |
| iPAN-*d* | 0.22 | 3.0 | 0.78 | 24.3 | 19.6 | 1.21 |
| DMA | 0.46 | 3.8 | 0.54 | 24.6 | 15.0 | |
| DEA | 0.35 | 4.1 | 0.65 | 36.9 | 25.4 | |
| DPA | 0.30 | 4.1 | 0.70 | 39.2 | 28.7 | |

[a] $\langle\tau_s\rangle = a_{s1}\tau_{s1} + a_{s2}\tau_{s2}$; $a_{s1} + a_{s2} = 1$.

**3.3. Solvation Dynamics.** Solvation dynamics are very important for detailed understanding of the ET dynamics.[7−15,43,44] The fluorescence decay shows spectral shift due to the stabilization by solvation and the spectral shift correlation function $C(t)$ is defined as

$$C(t) = \frac{\nu(t) - \nu(\infty)}{\nu(0) - \nu(\infty)} \tag{8}$$

where $\nu(t)$, $\nu(\infty)$, and $\nu(0)$ are the fluorescence peak frequencies at times $t$, $\infty$, and 0, respectively. We measure the solvation times of all the present electron donating solvents by the single-wavelength measurement method proposed by Barbara and coworkers.[45,46] It is based on a simple photodynamic model, in which it is assumed that the spectrum of the probe is a simple function of a single solvent parameter denoted as the solvent polarization. The fluorescence decay of the probe dye C102 is measured at the characteristic wavelength of 420 nm, and the fluorescence decay of C102 at this wavelength corresponds to the spectral shift correlation function.[45,46] Although this is not the best approximation to measure the solvation dynamics compared with the full constructed measurement, it is used for convenience in this study.

The obtained decays are analyzed by a triexponential function quite well where the longest decay time constant is fixed at 3 ns (the fluorescence lifetime of the probe in nonreactive solvents[40−42]). The other two decay time constants ($\tau_{s1}$ and $\tau_{s2}$) are considered due to the solvation dynamics for the respective solvents. The relative amplitudes of the two solvation components ($a_{s1}$ and $a_{s2}$) are given in a normalized form of $a_{s1} + a_{s2} = 1$. The obtained solvation parameters are listed in Table 2. In the table we also summarize an average solvation time, $\langle\tau_s\rangle$, and a ratio between $\langle\tau_s\rangle$ of normal and deuterated *N*-monoalkyl-

**TABLE 3: Reduction Potentials of Electron Acceptors and Oxidation Potentials of Electron Donors**

(A) Reduction Potentials of Coumarins in Acetonitrile, Aniline, and Amino-Deuterated Aniline

| | $E(\text{dye}^{0/-})$/mV vs SCE | | |
|---|---|---|---|
| solute | acetonitrile | AN[a] | AN-*d*2[a] |
| C151 | −1565 | −1640 | −1649 |
| C152 | −1626 | −1662 | −1671 |
| C481 | −1660 | −1658 | −1667 |
| C522 | −1653 | −1690 | −1701 |
| C153 | −1685 | −1710 | −1721 |

(B) Oxidation Potentials of Aniline Derivatives in $CH_3CN$, $CH_3OH$, and $CH_3OD$

| | $E(\text{solv}^{0/+})$/mV vs SCE | | |
|---|---|---|---|
| solute | $CH_3CN$ | $CH_3OH$ | $CH_3OD$ |
| AN[a] | +930 | +820 | |
| AN-*d*2[a] | +932 | | +838 |
| MAN | +810 | +726 | |
| MAN-*d* | +809 | | +734 |
| EAN | +804 | +718 | |
| EAN-*d* | | | +729 |
| nPAN | +801 | +709 | |
| nPAN-*d* | | | +718 |
| iPAN | +796 | +709 | |
| iPAN-*d* | +794 | | +719 |
| DMA | +756 | +715 | +722 |
| DEA | +719 | +682 | +689 |
| DPA | +722 | +672 | +683 |

[a] Reference 32.

anilines. Interesting points to be noted from Table 2 are (i) In *N*,*N*-dialkylanilines with bulkier alkyl groups the solvation dynamics are getting slower drastically, but in *N*-monoalkylanilines the solvation dynamics are almost independent of the size of the alkyl groups. (ii) The deuterium isotope effect on solvation dynamics of *N*-monoalkylanilines is almost independent of the size of the alkyl groups (∼20%). The present results show similar features to the AN[47] and methanol[48] cases.

Maroncelli and co-workers studied the solvation dynamics of substituted benzenes (benzonitrile, toluene, and others), and observed fast inertial components.[49,50] The fast dynamics of neat aniline derivatives have been studied by the optical Kerr effect.[51,52] In the present work, the effect of the inertial component on the ET dynamics is included in the 2D-ET model.

**3.4. Reduction Potentials of Coumarin Dyes and Oxidation Potentials of Electron Donating Solvents.** The reduction and oxidation potentials are measured and summarized in Table 3. The reduction potential of C151 is highest and that of C153 is lowest. These results indicate that C151 is most reductive and C153 is most stable among the coumarins used in the present study. From the oxidation potentials of the electron donors in acetonitrile, it is seen that the aniline derivative which has a larger alkyl group is a stronger electron donor. This tendency can be interpreted in terms of the plus inductive (+I) effect: propyl group > ethyl group > methyl group > hydrogen, and *N*,*N*-dialkyl groups > *N*-monoalkyl group > hydrogens. To estimate the deuterium isotope effect of the redox potentials in the hydrogen-bonding liquids, the oxidation potentials of the donor molecules in methanol and deuterated methanol ($CH_3OD$) are measured and are also listed in Table 3B. Interestingly, the oxidation potentials of the donor molecules in deuterated methanol are about 10 mV higher than those in normal methanol. We already reported[32] that the reduction potentials of the coumarin dyes in AN-d2 are about 10 mV lower than those in normal AN (Table 3A).

## 4. Estimation of the Free Energy Gap $\Delta G^0$

To perform a quantitative discussion on the ET dynamics, it is necessary to obtain reliable values of $\Delta G^0$. However, in some ET systems it is very difficult to estimate $\Delta G^0$ accurately. That is especially true for ET reaction in the excited state where three electronic states, the ground state, locally excited state, and charge transfer state, are associated with the reaction.[53] Normally, one can estimate $\Delta G^0$ for the excited-state ET in a polar solvent by the following relationship,[54]

$$\Delta G^0 = -E_{00} + E(\text{donor}^{0/+}) - E(\text{acceptor}^{0/-}) - E_{\text{IPS}} \qquad (9)$$

where, $E_{00}$ is the energy difference between the $S_0$ and $S_1$ states, $E(\text{donor}^{0/+})$ is the oxidation potential of the electron donor, $E(\text{acceptor}^{0/-})$ is the reduction potential of the electron acceptor, and $E_{\text{IPS}}$ is the ion pair stabilization energy.

In less polar solvents such as AN or DMA, however, it is much more complicated to estimate $\Delta G^0$ by the eq 9 than in polar solvent. That is because reliable electrochemical measurement is fairly difficult due to small solubility of electrolyte in the solvents. In such solvents electrolyte molecules may form aggregates. One possible way to obtain $\Delta G^0$ in a less polar solvent is to extrapolate the $\Delta G^0$ value from those in a polar solvent with the help of an equation on dielectric interaction such as the Born equation.[55−57] In this work we extrapolate the $\Delta G^0$ values by an empirical equation for dielectric interaction energy suggested by Fawcett.[58,59]

Further, we try to include the effect of molecular size more explicitly because the substituent effect of the donor causes changes of the dimension of the molecule and several ET parameters such as $\Delta G^0$ and $V_{\text{el}}$ depend on the molecular size more or less. Here, we invoke a very simple model for the molecular dimension of which a spherical shape is assumed for the molecule. The molecular volume is estimated in terms of a sum of the van der Waals volumes of the constituent atoms. Since the structures of the anilines and coumarins are undoubtedly more complicated than can be predicted by this model, the simulations should be taken as only suggestive of the real behavior.

Among the ET parameters which are influenced by the molecular dimension, $\Delta G^0$ is rather insensitive to it. Even we employ a different model for the molecular size, the predicted $\Delta G^0$ values are not changed so much. On the other hand, $V_{\text{el}}$ is expected to depend on the intermolecular distance very much. In the later section we will show that this spherical model cannot provide a sufficiently accurate values for $V_{\text{el}}$. However, we think that $\Delta G^0$ can be evaluated by this model moderately well.

$E_{00}$ is estimated from the crossing point of the normalized absorption and fluorescence spectra of the coumarins in the respective solvents. $E_{\text{IPS}}$ is estimated by the equation

$$E_{\text{IPS}} = \frac{e^2}{\epsilon_s l} \qquad (10)$$

where $e$ is the electronic charge, $\epsilon_s$ is the dielectric constant of solvent, and $l$ is the distance between the donor and acceptor molecules. To estimate $l$, we calculate a crude molecular volume, $V$, from atomic increments.[60] A molecule is assumed as a spherical shape, therefore the radius $r$ of the donor molecule and the acceptor molecule is estimated from the calculated molecular volume $r = (3V/4\pi)^{1/3}$. In the present systems the solvent is the electron donor, therefore we consider that the distance between the acceptor and donor is a sum of the radii of the acceptor and donor molecules.

**TABLE 4: Empirical Solvent Parameters of AN, MAN, DMA, and $CH_3CN$**

| | $\epsilon_s$[a] | Dn[b] | Bp | $E_T(30)$[c] | Ap |
|---|---|---|---|---|---|
| AN | 6.86 | 35 | 13.9 | 44.3 | 23.8 |
| MAN | 5.97 | 33 | 13.7 | 42.5 | 21.5 |
| DMA | 5.11 | 27 | 13.1 | 36.5 | 13.8 |
| $CH_3CN$ | 37.5 | 14 | 11.7 | 45.6 | 25.5 |

[a] References 30 and 65. [b] Reference 64. [c] Reference 63.

$$l = r(\text{donor}) + r(\text{acceptor}) \tag{11}$$

The reduction potentials of the coumarins and the oxidation potentials of the solvents are measured in acetonitrile in the present work. We use the empirical relations between solvation energy and solvent polarity to extrapolate the redox potentials from that in polar solvents to that in less polar solvents. Fawcett proposed an equation for solvation energy with empirical parameters which are estimated from solvent acidity and basicity.[58,59] The solvation energy of halide ion ($G_s^0(-)$) is given by

$$G_s^0(-) = -\left(\frac{N_0 z_i^2 e^2}{8\pi\epsilon_0}\right)\left(1 - \frac{1}{\epsilon_s}\right)\left(\frac{1}{\frac{1}{\text{Ap}} + r_i}\right) \tag{12}$$

and that of alkali metal cation ($G_s^0(+)$) is given by

$$G_s^0(+) = -\left(\frac{N_0 z_i^2 e^2}{8\pi\epsilon_0}\right)\left(1 - \frac{1}{\epsilon_s}\right)\left(\frac{1}{\frac{1}{\text{Bp}} + r_i}\right) \tag{13}$$

where $N_0$ is the Avogadro's number, $z_i$ is the ionic charge, $e$ is the electronic charge, $\epsilon_0$ is the permittivity of free space, $\epsilon_s$ is the dielectric constant of solvent, $r_i$ is the ionic radius, and Ap and Bp are the Fawcett's solvent parameters of acidity and basicity, respectively. Ap and Bp are defined by the following equations

$$\text{Ap} = 1.29E_T(30) - 33.3 \tag{14}$$

$$\text{Bp} = 10.14 + 0.108\text{Dn} \tag{15}$$

where $E_T(30)$ is the polarity scale which is defined by Dimroth et al.,[61] and Dn is the donor number defined by Gutmann.[62] $E_T(30)$,[63] Dn,[64] Ap, Bp, and the dielectric constant[30,65] of AN, MAN, and DMA are summarized in Table 4. We use the empirical relationship for estimation of the difference of the solvation energies in acetonitrile and aniline derivatives ($\Delta G_s^0$). Namely,

$$\Delta E_{sol} = \Delta G_s^0(-) + \Delta G_s^0(+) \tag{16}$$

Here, we use the radius of neutral molecule for $r_i$. Equation 9 is rewritten by

$$\Delta G^0 = -E_{00} + (E(\text{sol}^{0/+})_{\text{in acetonitrile}} - E(\text{dye}^{0/-})_{\text{in acetonitrile}} + \Delta E_{sol}) - E_{IPS} \tag{17}$$

The obtained values of $E_{00}$, $l$, $E_{IPS}$, $\Delta E_{sol}$, and $\Delta G^0$ are listed in Table 5. For estimation of $E_{IPS}$ and $\Delta E_{sol}$ of *N*-monoalkylanilines, we use the values ($\epsilon_s$, $E_T(30)$, and Dn) of MAN. For *N*,*N*-dialkylanilines, we use those of DMA.

## 5. Simulation of the Electron-Transfer Dynamics: 2D-ET Model

**5.1. Theoretical Background.** According to the prediction of the conventional ET theories (eq 6), the ET dynamics should be either slower than or almost equal to the solvation process. However, for the present systems some ET occurs much faster than the solvation dynamics. Furthermore, the present ET dynamics show nonexponential behavior. We used the two-dimensional ET model[33−36] to explain these ultrafast ET dynamics. In this model the intramolecular vibrational motion is separately treated from the solvation dynamics. Here we also adopt the two-dimensional model in order to rationalize the experimental results. In this section we briefly outline the theoretical framework of the model and explain how to estimate the ET parameters.

Figure 7a shows a conceptual picture for the 2D-ET model on the present cases. The ET reaction occurs along the nuclear coordinate $q$, and the motion along the $q$ coordinate is considered to be very fast in comparison to that along the solvent coordinate, $X$. The reaction along the $q$ coordinate is a function of the vibrational modes of the system and is treated classically. Walker et al.[66] considered a high-frequency accepting mode ($\nu_h$) of the product in the 2D-ET model and treated it in a same way as that by Jortner and Bixon.[69] Figure 7b is the scheme of ET process based on this extended model. Here, it is assumed that the curvatures of the free energy surfaces in each vibrational level ($n$) along both $q$ and $X$ coordinates are the same. The free energy functions of the reactant and product states are thus given by[66]

$$G_r(X,q) = \lambda_s X^2 + \lambda_l q^2 \tag{18}$$

$$G_p(X,q,n) = \lambda_s(X-1)^2 + \lambda_l(q-1)^2 + nh\nu_h + \Delta G^0 \tag{19}$$

where the free energy function is assumed to be the quadratic function of both $q$ and $X$ according to the linear response theory, and these coordinates are normalized, that is, the $X$ and $q$ coordinates are (0,0) and (1,1) for the bottoms of the reactant and the product states, respectively. $\lambda_s$ is the solvent reorganization energy (for the $X$ coordinate), $\lambda_l$ is the nuclear reorganization energy (for the $q$ coordinate), and $\nu_h$ is the frequency of the high-frequency vibrational mode coupled to the ET.

With this picture the motion of the population along $X$ can be expressed by the following diffusion-reaction equation[33−36]

$$\frac{\partial p(X,t)}{\partial t} = D(t)\frac{\partial}{\partial X}\left[\frac{\partial}{\partial X} + \frac{1}{k_B T}\frac{dG_r(X)}{dX}\right]p(X,t) - \sum_n k(n,X)p(X,t) \tag{20}$$

where $p(X,t)$ is the classical probability distribution function at $X$ and $t$, $G_r(X)$ is the free energy of the reactants at the $X$ coordinate, which is equal to $\lambda_s X^2$, and $D(t)$ is the time-dependent diffusion coefficient and is expressed by[68]

$$D(t) = -\frac{k_B T}{2\lambda_s}\frac{1}{\Delta(t)}\frac{d\Delta(t)}{dt} \tag{21}$$

where $\Delta(t)$ is the time-correlation function of the solvent coordinate, which is equal to the spectral shift correlation function $C(t)$ and is expressed as,[68]

$$\Delta(t) = C(t) = \sum_n a_n \exp\left(-\frac{t}{\tau_{sn}}\right) \tag{22}$$

where $\tau_{sn}$ is the time constant of the $n$th component of the solvation and $a_n$ is the corresponding amplitude $\sum_n a_n = 1$. In

**TABLE 5: Absorption and Fluorescence Maxima and $\Delta G^0$ Parameters[a]**

| acceptor | donor | $\lambda_{abs}$/nm | $\lambda_{fl}$/nm | $E_{00}$/eV | $l$/Å | $E_{ISP}$/eV | $\Delta E_{sol}$/eV | $\Delta G^0$/eV |
|---|---|---|---|---|---|---|---|---|
| C151 | AN | 377 | 462 | 3.03 | 6.15 | 0.34 | 0.41 | −0.47 |
| | MAN | 373 | 440 | 3.05 | 6.31 | 0.38 | 0.52 | −0.54 |
| | EAN | 372 | 435 | 3.06 | 6.46 | 0.37 | 0.51 | −0.56 |
| | nPAN | 371 | 432 | 3.07 | 6.59 | 0.37 | 0.50 | −0.57 |
| | iPAN | 370 | 440 | 3.08 | 6.59 | 0.37 | 0.50 | −0.59 |
| | DMA | 370 | 410 | 3.11 | 6.46 | 0.44 | 0.73 | −0.50 |
| | DEA | 370 | 413 | 3.15 | 6.72 | 0.42 | 0.71 | −0.58 |
| | DPA | 369 | 414 | 3.15 | 6.94 | 0.41 | 0.70 | −0.57 |
| C152 | AN | 410 | 503 | 2.77 | 6.39 | 0.33 | 0.40 | −0.14 |
| | MAN | 405 | 468 | 2.79 | 6.55 | 0.37 | 0.49 | −0.23 |
| | EAN | 403 | 466 | 2.81 | 6.70 | 0.36 | 0.49 | −0.25 |
| | nPAN | 402 | 465 | 2.82 | 6.83 | 0.35 | 0.48 | −0.27 |
| | iPAN | 400 | 466 | 2.83 | 6.83 | 0.35 | 0.48 | −0.28 |
| | DMA | 396 | 446 | 2.86 | 6.70 | 0.42 | 0.69 | −0.21 |
| | DEA | 396 | 451 | 2.87 | 6.96 | 0.41 | 0.68 | −0.25 |
| | DPA | 392 | 460 | 2.89 | 7.18 | 0.39 | 0.67 | −0.26 |
| C481 | AN | 413 | 502 | 2.73 | 6.59 | 0.32 | 0.39 | −0.07 |
| | MAN | 410 | 464 | 2.75 | 6.75 | 0.36 | 0.48 | −0.16 |
| | EAN | 408 | 465 | 2.77 | 6.90 | 0.35 | 0.47 | −0.19 |
| | nPAN | 407 | 467 | 2.78 | 7.03 | 0.34 | 0.47 | −0.19 |
| | iPAN | 406 | 467 | 2.78 | 7.03 | 0.34 | 0.47 | −0.20 |
| | DMA | 398 | 448 | 2.85 | 6.90 | 0.41 | 0.67 | −0.17 |
| | DEA | 398 | 455 | 2.85 | 7.16 | 0.39 | 0.65 | −0.21 |
| | DPA | 398 | 456 | 2.85 | 7.38 | 0.38 | 0.64 | −0.21 |
| C522 | AN | 423 | 513 | 2.67 | 6.52 | 0.32 | 0.39 | −0.02 |
| | MAN | 419 | 502 | 2.69 | 6.68 | 0.36 | 0.48 | −0.11 |
| | EAN | 417 | 500 | 2.70 | 6.83 | 0.35 | 0.47 | −0.12 |
| | nPAN | 415 | 496 | 2.72 | 6.96 | 0.35 | 0.47 | −0.14 |
| | iPAN | 414 | 495 | 2.72 | 6.96 | 0.35 | 0.47 | −0.15 |
| | DMA | 408 | 463 | 2.77 | 6.83 | 0.41 | 0.68 | −0.09 |
| | DEA | 406 | 460 | 2.78 | 7.09 | 0.40 | 0.66 | −0.15 |
| | DPA | 406 | 468 | 2.80 | 7.31 | 0.39 | 0.65 | −0.16 |
| C153 | AN | 435 | 530 | 2.58 | 6.68 | 0.32 | 0.38 | +0.10 |
| | MAN | 430 | 515 | 2.61 | 6.84 | 0.35 | 0.47 | 0.00 |
| | EAN | 430 | 511 | 2.61 | 6.99 | 0.35 | 0.47 | 0.00 |
| | nPAN | 428 | 505 | 2.63 | 7.12 | 0.34 | 0.46 | −0.02 |
| | iPAN | 427 | 505 | 2.63 | 7.12 | 0.34 | 0.46 | −0.03 |
| | DMA | 416 | 504 | 2.71 | 6.99 | 0.40 | 0.66 | −0.01 |
| | DEA | 416 | 504 | 2.71 | 7.25 | 0.39 | 0.64 | −0.06 |
| | DPA | 418 | 503 | 2.70 | 7.47 | 0.38 | 0.63 | −0.04 |

[a] Transition energy $E_{00}$, distance $l$, ion stabilization energy $E_{IPS}$, and free energy gap $\Delta G^0$.

the present work the observed solvation dynamics can be reproduced well in terms of a sum of two exponentials. $k(n,X)$ is the $X$ coordinate dependent reaction rate constant for the $n$th high-frequency vibrational state of the product. The reaction rate constant $k(n,X)$ is expressed as[14,31,32,66]

$$k(n,X) = \frac{2\pi(V_{el,n})^2}{\hbar\sqrt{4\pi\lambda_l k_B T}} \exp\left(-\frac{\Delta G^*(n,X)}{k_B T}\right) \qquad (23)$$

where $V_{el,n}$ is the electronic matrix element between the vibrational ground state of the reactant and the $n$th vibrational state of the product and is expressed by the Franck−Condon factor as

$$V_{el,n}{}^2 = V_{el}{}^2|\langle 0|n\rangle|^2 = V_{el}{}^2\{(S^n/n!)\exp(-S)\} \qquad (24)$$

where $S = \lambda_h/h\nu_h$ is the electron-vibrational coupling strength and $\lambda_h$ is the reorganization energy for the high-frequency mode. $\Delta G^*(n,X)$ is the activation energy for the $n$th vibrational state and is written by[14,31,32,66]

$$\Delta G^*(n,X) = \frac{(\lambda_s + \Delta G^0 - 2\lambda_s X + nh\nu_h + \lambda_l)^2}{4\lambda_l} \qquad (25)$$

The method to estimate the ET parameters will be described in the following section.

In the simulation of the ET dynamics, we first solve the diffusion-reaction equation (eq 20) numerically to obtain the time-dependent probability $p(X,t)$. We next calculate the time-resolved emission spectra using the time-dependent probability and steady-state emission spectrum in a nonpolar solvent.[31,32] The time-resolved fluorescence spectra are expressed as[69]

$$I(\nu,t) = \int_{-\infty}^{+\infty} |M|^2 g[\nu_0(X),\{\nu - \nu_0(X)\}]p(X,t)\nu^3 \, dX \qquad (26)$$

where $I(\nu,t)$ is the fluorescence intensity at frequency $\nu$ and time $t$, $|M|^2$ is the square of the electronic transition moment matrix element, $\nu_0(X)$ is the frequency corresponds to the energy gap at the solvent coordinate $X$ (i.e., $\nu_0(X) = [F_{s1}(X) - F_{s0}(X)]/h$), where $F_{s1}$ and $F_{s0}$ are the free energy functions for the $S_1$ and $S_0$ states, respectively. $g[\nu_0(X), \{\nu - \nu_0(X)\}]$ is the normalized vibrational shape function of the emission band. The last function corresponds to the Franck−Condon factors for the vibrational sequences and progressions in the spectrum. In this simulation, the function $g[\nu_0(X), \{\nu - \nu_0(X)\}]$ is empirically assumed to be equal to the emission spectra of the dyes in cyclohexane. Finally, the fluorescence decay at the corresponding wavelength is observed from this time-resolved spectrum, which is plotted in the following figures (Figures 8, 10, 13, 14, and 15 *vide infra*). In this model, both the time-dependent probability and the decay at the single wavelength show highly nonexponential features, just as we observed.[31,32]

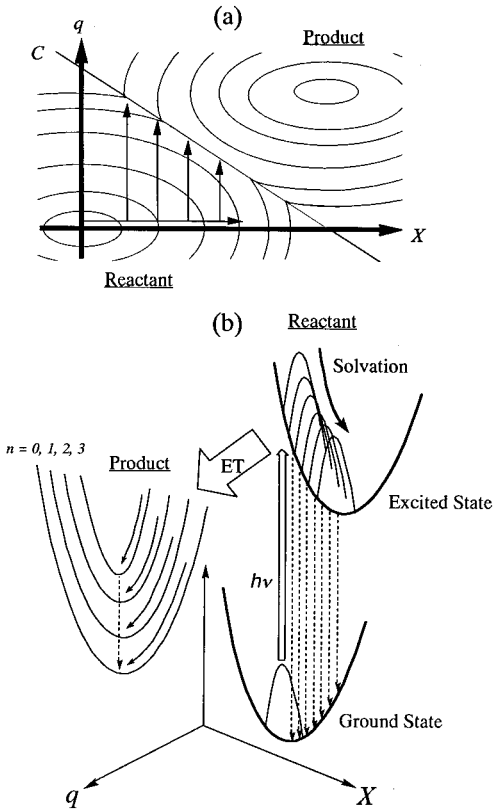


**Figure 7.** (a) Two dimensional description of potentials of electron transfer reaction with solvent coordinate ($X$) and nuclear coordinate ($q$). Curve C indicates the transition state. (b) Conceptual scheme of electron transfer in competition with solvent relaxation process in the excited state. Solvent relaxation occurs on the $X$ coordinate and electron transfer occurs on the $q$ coordinate.

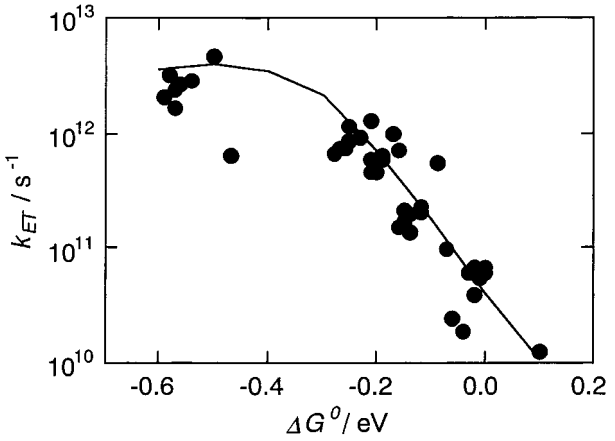


**Figure 8.** Plot of the experimental (circle) and simulated (solid line) average rate constants of electron transfer ($k_{ET}$) vs the free energy gap ($\Delta G^0$). Simulation is based on the two-dimensional electron transfer model. The parameters for electron transfer are $\lambda_s = 1300$ cm$^{-1}$, $\lambda_h = 2000$ cm$^{-1}$, $\lambda_l = 2200$ cm$^{-1}$, $\nu_h = 1400$ cm$^{-1}$, and $V_{el} = 130$ cm$^{-1}$.

At the end of this section, let us briefly mention about the relation between ET dynamics and $\Delta G^0$. Since most of the ET dynamics we investigate are faster than or similar to the solvation process, the original Marcus theory[18,19] on ET cannot be applied to the present systems. That is because the original Marcus theory assumes that motions of solvent molecules are very much faster than ET. However, as already shown,[31,32] the dependence of the ET rate on $\Delta G^0$ shows a "bell-shape" feature even in the 2D-ET model, which is often seen in the cases predicted by the original Marcus theory. Therefore, we use the common terminology to express the relation between the ET rate and $\Delta G^0$ such as "normal region", "barrierless region", or "inverted region".

**5.2. ET Parameters for Simulation.** First, we discuss about the solvent reorganization energy. To normalize the reaction coordinate, the bottom of the reactant state ($S_1$ state of coumarin) puts at $(X,q) = (0,0)$ and that of the product state puts at $(X,q) = (1,1)$. The bottom of the ground-state free energy surface ($S_0$ state of coumarin) is assumed to be at $(X,q) = (0.4,0)$ in the simulation similarly to before.[32] The reorganization energy for the solvent ($\lambda_s$) is estimated by the following equation:[32]

$$2\lambda_s X^2 = \Delta\nu \tag{27}$$

$\Delta\nu$ is roughly estimated from the differences of the steady-state Stokes shift of C102 in a nonpolar solvent, cyclohexane (3090 cm$^{-1}$), and in MAN (3490 cm$^{-1}$). $\Delta\nu$ is estimated to be 400 cm$^{-1}$, and the calculated $\lambda_s$ is 1300 cm$^{-1}$. We use this value for all the simulations we perform since the dielectric constants are quite the same for all the solvents.

The next parameter we consider is the high-frequency vibrational mode, $\nu_h$, coupled to the ET reaction. One of such modes could be the nitrogen-phenyl ring carbon (N−Ph) stretching mode of aniline derivatives. The oxidation reaction of aniline occurs at the lone pair electrons of the nitrogen atom.[70] The N−Ph stretching mode of aniline derivative is very important during the reaction because of the change of the molecular structure (from the $sp^3$ orbital to the $sp^2$ orbital):

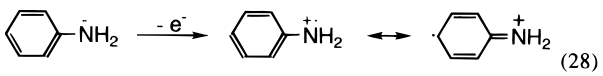

(28)

According to the reported IR and Raman results[71−73] in some aniline derivatives (radical cation form), the frequency of this stretching vibrational mode for AN, DMA, and DEA is 1494, 1366, and 1421 cm$^{-1}$, respectively. Here we tentatively choose 1400 cm$^{-1}$ for all the simulations, since even we use the above values the simulation results are not appreciably changed.

As for the solvation dynamics parameters ($a_{s1}$, $a_{s2}$, $\tau_{s1}$, and $\tau_{s2}$) and the free energy gap $\Delta G^0$, the values experimentally obtained are used. Other ET parameters such as the electronic matrix element $V_{el}$ and reorganization energies of the high- and low- frequency modes ($\lambda_h$ and $\lambda_l$) are optimized so that the simulation reproduces the experimental results and the parameters are in the physical reasonable range.

## 6. Discussion

In the previous studies, we investigated the substituent effect[31] of the acceptor molecule and the deuterium isotope effect[32] on the ET dynamics in the coumarin-aniline system. From the research of substituent effect of the 7-amino coumarins,[31] it was found that the ET rate strongly depends on the amino group of the coumarin. The drastic change of the ET rate mainly comes from the electron-accepting ability of the coumarin dye. The study of the isotope substitution effects on ET showed following points:[32] (i) Clear deuterium isotope effects on the ET rates have been observed in the case of AN, but not in DMA. (ii) No isotope substitution effect of coumarin (amino hydrogen (C151) and dimethyl hydrogens (C152)) on the ET has been observed. It was concluded that the isotope effect of AN on the ET mostly arises from the difference of $\Delta G^0$ due to the stabilization energies of the normal and deuterated hydrogen-bonding interaction of AN as a solvent.

**6.1. General Features of Substituent Effect of the Donor.** It is clear that for the present systems the ET dynamics depend

drastically on the substituent amino groups of both the donor solvents and acceptor coumarin dyes (Figures 2, 4, and 5). The substituent effect of the coumarin dyes on the ET dynamics can be discussed by a number of possible causes, such as the free energy gap ($\Delta G^0$), the frequencies of the vibrational modes, and others. In our earlier studies[32] the effect of isotope substitutions of the acceptor dyes at the 7-amino group was not evident. The result thus may indicate that the vibrational motions of the 7-amino group of the coumarin dyes is not coupled to the ET dynamics.

The energy difference between the $S_0$ and $S_1$ states $E_{00}$ is different at each coumarin−aniline combination. The excitation wavelength is fixed at 400 nm in the present work. The different excess vibrational energy might affect the ET dynamics by the vibrational relaxation. However, the excitation wavelength dependence of the ET dynamics has not been observed within the experimental accuracy.[74] This means that the ET dynamics is insensitive to the vibrational relaxation in this experiment. Though more detailed studies might be needed at higher time resolution, we ignore the effect in the present study.

Let us summarize the experimental results briefly. It is evident from the comparison of the experimental results on ET and solvation dynamics (Tables 1 and 2) that in many of the present systems the ET dynamics is faster than the solvation process. Thus in all the electron donating solvents, except for in AN, the fast component of the ET process ($\tau_1$, Table 1) for C151, C152, C481, and C522 are faster than the fast component of the solvation process ($\tau_{s1}$, Table 2). The second component of the ET process ($\tau_2$, Table 1) is, however, slower than the fast component of the solvation process ($\tau_{s1}$, Table 2). More interestingly, for C151, in all the electron-donating solvents, except for that in AN, the ET process is extraordinarily fast, so that even the slow component of the ET process ($\tau_2$, Table 1) is faster than the fast component of the solvation process ($\tau_{s1}$, Table 2). The results thus indicate that in most of the present systems the fast part of ET process is hardly influenced by the solvent dynamic nature. The slower part of the ET process, however, seems to be influenced by the solvent property.

Now let us see the general features of the substituent effect of the donor on the ET dynamics, we summarize the experimental results in Scheme 1. The ET in AN is slowest, and *N*,*N*-dialkylanilines provides faster ET than *N*-monoalkylanilines. *In a series of N-monoalkylanilines the ET rate does not depend on the alkyl group appreciably. In contrast to this, the ET rate in N,N-dialkylanilines strongly depends on the alkyl group; the larger the alkyl group is, the slower the ET is.*

Figure 8 shows the average ET rates of all the systems as a function of $\Delta G^0$ (circles). From the figure it is seen that the ET dynamics becomes faster as the absolute value of $\Delta G^0$ increases. This suggests that all the experimental data can be simulated with a single set of the ET parameters. We calculate the ET rates (fluorescence decay rates) by means of the 2D-ET model with the following parameters; $\lambda_h = 2000$ cm$^{-1}$, $\lambda_l = 1400$ cm$^{-1}$, and $V_{el} = 130$ cm$^{-1}$. The calculated result is shown in the figure (line), and it is clear that the simulation reproduces the general trend of the experimental data moderately well. However, if we closely observe the ET dynamics in different aniline homologues, we see an interesting characteristic nature. In the following sections we discuss the substituent effects for the individual cases in more detail.

**6.2. Aniline, *N*-Methylaniline, and *N*,*N*-Dimethylaniline.** We discuss the difference of the ET rate in AN, MAN, and DMA. The average ET rates in AN, MAN, and DMA are plotted as a function of the free energy gap ($\Delta G^0$) in Figure 9.

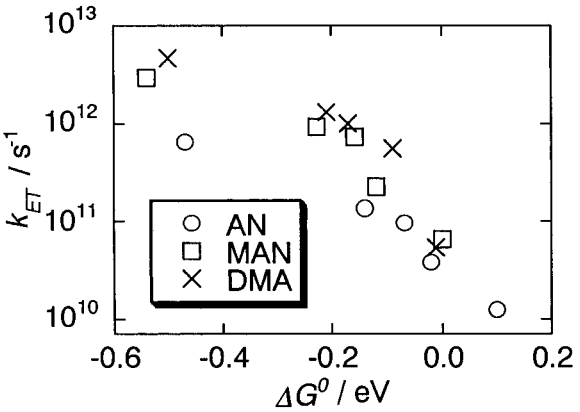


**Figure 9.** Plot of the experimentally obtained electron transfer rate constants ($k_{ET}$) in AN (○), MAN (□), and DMA (×) vs the free energy gap ($\Delta G^0$). $k_{ET}$ is defined as the inverse of the average lifetime of the coumarin ($\langle\tau\rangle$). $\Delta G^0$ is obtained from eq 17.

**SCHEME 1. Relationship of the ET Rate Constants of the Electron Donating Solvents of Aniline, *N*-Monoalkylanilines, and *N*,*N*-Dialkylanilines**

$$k_{ET}\,(\mathrm{AN})$$

$$\wedge\!\wedge$$

$$k_{ET}\,(\mathrm{MAN}) \sim k_{ET}\,(\mathrm{EAN}) \sim k_{ET}\,(\mathrm{nPAN}) \sim k_{ET}\,(\mathrm{iPAN})$$

$$\wedge$$

$$k_{ET}\,(\mathrm{DMA}) \;>\; k_{ET}\,(\mathrm{DEA}) \;>\; k_{ET}\,(\mathrm{DPA})$$

The important points to be noted are (i) For all the coumarins, except for C153, the ET rate increases in order of $k_{ET}$(AN) ≪ $k_{ET}$(MAN) < $k_{ET}$(DMA). For C153, however, the order is $k_{ET}$(AN) ≪ $k_{ET}$(DMA) ≤ $k_{ET}$(MAN). (ii) Roughly, all the plots seem to lie on a single curve of $k_{ET}$ vs $\Delta G^0$. However, on closer examination, it can be seen that the curve for DMA is greater than that of AN. (iii) All the curves fall in the normal and barrierless regions.

It is seen from Table 5 that for each coumarin the $\Delta G^0$ value of AN is the most positive and that of MAN is similar to that of DMA. However, it is clear from Figure 9 that the ET rate in DMA is faster than that in MAN despite almost the same $\Delta G^0$, and the ET rate in DMA and MAN is much faster than that in AN despite the small differences between $\Delta G^0$ of AN and DMA or MAN. The results indicate that some ET parameters in three solvents have different values. Especially, the maximum $k_{ET}$ of AN is smaller than that of DMA and MAN.

The magnitude of the maximum $k_{ET}$ is mostly determined by $V_{el}$. Here, we consider that the difference in the intermolecular distance is caused by the different values of $V_{el}$. One of the most simple forms of the dependence of $V_{el}$ on the intermolecular distance can be expressed as[6]

$$V_{el} = V_{el0} \exp[-\beta(l - l_0)/2] \qquad (29)$$

where $V_{el0}$ the distance-independent electronic matrix element, namely the electronic matrix element for a donor−acceptor pair at van der Waals separation $l_0$. $l$ is the separation between the donor and acceptor sites, and $\beta$ is a constant scaling the distance dependence of $V_{el}$. It is clear from eqs 29 and 23 that a longer distance between the donor and acceptor gives a smaller maximum $k_{ET}$. However, the experimental results are not explained by the difference in distance (AN is the smallest molecule and DMA is the largest molecule but the maximum $k_{ET}$ of AN is smallest and that of DMA is largest). This should

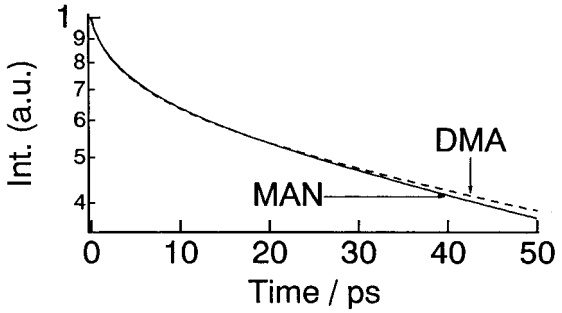


**Figure 10.** Comparison of the simulated single-wavelength decays of C153 in MAN (solid line) and DMA (broken line). The different parameter is the solvation time. The electron transfer rate in the timescale is affected by the solvation dynamics.

indicate that the distance-independent electronic matrix elements, $V_{el0}$ of AN, MAN, and DMA are quite different:$V_{el0}$(DMA) > $V_{el0}$(MAN) > $V_{el0}$(AN). The other parameters ($\nu_h$, $\lambda_h$, and so on) should be changed by the different alkyl group, but the experimental $k_{ET}$ vs $\Delta G^0$ relations are not fitted by changing the other ET parameters in the physically reasonable range. This suggests that the different maximum $k_{ET}$ is mainly arising from the $V_{el0}$.

$V_{el}$ is not only dependent on the distance of the donor−acceptor pair but also is the relative orientation between donor and acceptor. In the present system the acceptor molecule is surrounded by many donor molecules. Thus the most efficient ET should occur at the most suitable orientation. The orientation may be slightly different in the each coumarin and aniline system and it may affect on $V_{el0}$. This could also be a reason that $V_{el0}$ is different in different solvents.

As mentioned in section 3.1.1., the ET rates of the slowest dye, C153, are quite similar to the inverse of the solvation time for both MAN and DMA (Tables 1 and 2). It is seen from Table 2 that the solvation dynamics of DMA is *slower* than that of MAN. It may thus be interpreted that because of the slower solvation dynamics of DMA, the ET rate in C153/DMA could be slower than that in C153/MAN, as we observe experimentally. Figure 10 shows the result of the simulation on the effect of the difference of the solvation times. In this simulation, we consider C153 in MAN and DMA to estimate how the solvation dynamics affects on the ET dynamics in the time scale. All the ET parameters are fixed except for the solvation time ($a_{s1} = 0.25$, $\tau_{s1} = 2.0$ ps, $a_{s2} = 0.75$, and $\tau_{s2} = 16.2$ ps for MAN and $a_{s1} = 0.46$, $\tau_{s1} = 3.8$ ps, $a_{s2} = 0.54$, and $\tau_{s2} = 24.6$ ps for DMA) because of the difference of $\Delta G^0$ is very small. It is shown from this figure that ET in MAN is faster than in DMA (about 10% on $\langle\tau\rangle$). This means that an ET on this time scale is strongly affected by the solvation dynamics and the experimental result is qualitatively consistent with the simulation.

**6.3. *N*-Monoalkylanilines and *N,N*-Dialkylanilines.** The average ET rate constants in *N*-monoalkylanilines are plotted against $\Delta G^0$ in Figure 11. The interesting point to be noted from this figure is that the $k_{ET}$ vs $\Delta G^0$ relations are almost identical for all the *N*-monoalkylanilines. These results show that the ET parameters in *N*-monoalkylanilines are very similar and are not much dependent on the nature of the alkyl group in *N*-monoalkylanilines.

In contrast to the *N*-monoalkylanilines, the $\Delta G^0$ dependence of $k_{ET}$ for *N,N*-dialkylanilines differs with each other as shown in Figure 12. The magnitude with DMA as the donor solvent is largest and that with DPA as the donor solvent is smallest. As mentioned in section 6.1., these differences may be come

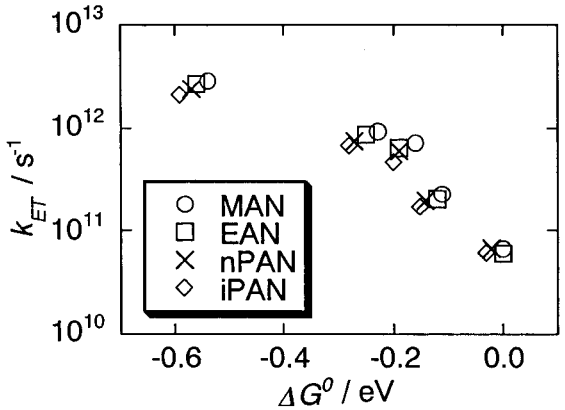


**Figure 11.** Plot of the experimentally obtained electron transfer rate constants ($k_{ET}$) in *N*-monoalkylanilines, MAN (○), EAN (□), nPAN (×), and iPAN (◇) vs free energy gap ($\Delta G^0$). $k_{ET}$ is defined as the inverse of the average lifetime of the coumarin ($\langle\tau\rangle$). $\Delta G^0$ is obtained from eq 17.

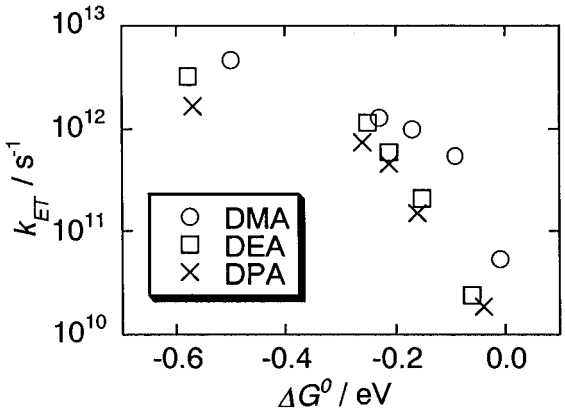


**Figure 12.** Plot of the experimentally obtained electron transfer rate constants ($k_{ET}$) in *N,N*-dialkylanilines, DMA (○), DEA (□), and DPA (×) vs free energy gap ($\Delta G^0$). $k_{ET}$ is defined as the inverse of the average lifetime of the coumarin ($\langle\tau\rangle$). $\Delta G^0$ is obtained from eq 17.

from $V_{el}$, and the trend of the magnitude of $V_{el}$ is $V_{el}$(DMA) > $V_{el}$(DEA) > $V_{el}$(DPA).

The electronic matrix element can be expressed as an exponential function of the separation between the donor and acceptor sites (eq 29). In the present systems the electron donors are the aniline derivative and the N-atom of anilines would be the actual site for electron donation (having a lone electron pair on the N-atom).[70] As the larger alkyl groups are substituted to the amino group of aniline, it is expected that it will cause a larger separation between the donor and acceptor sites, resulting in a reduction in $V_{el}$ and hence $k_{ET}$ will be reduced. The trend is clearly indicated for the series of *N,N*-dialkylanilines.

Figure 13 shows the best fits of $k_{ET}$ vs $\Delta G^0$ for DMA and DPA. Two curves seem to be vertically shifted. $V_{el}$ is optimized by the fitting, without changing the other ET parameters for both cases. The simulation results and experimental data are in good agreement. The obtained $V_{el}$ values in *N,N*-dialkylanilines are in order of $V_{el}$(DMA) > $V_{el}$(DEA) > $V_{el}$(DPA). This tendency is consistent with the change of the molecular radii. Because the primary step of the oxidation reaction of aniline occurs on the nitrogen atom (eq 28),[70] it should be considered that the larger alkyl group on the nitrogen atom is strongly affected by the distance between the donor and acceptor for the series of dialkylanilines. As it is clear from eq 29, the longer distance makes $V_{el}$ smaller.

However, the alkyl substituent effect on the ET dynamics in *N*-monoalkylanilines is not observed. This is not expected from

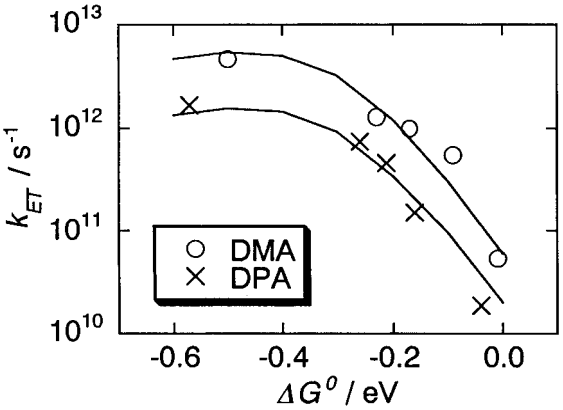


**Figure 13.** Best fits for the average electron transfer rate constants ($k_{ET}$) in DMA and DPA vs free energy gap ($\Delta G^0$). The experimental data of DMA and DPA are circle and cross, respectively. The parameters for electron transfer are $\lambda_s = 1300$ cm$^{-1}$, $\lambda_h = 1900$ cm$^{-1}$, $\lambda_l = 2100$ cm$^{-1}$, $\nu_h = 1400$ cm$^{-1}$, and $V_{el} = 150$ (DMA) and 80 cm$^{-1}$ (DPA). The different parameter between DMA and DPA is only $V_{el}$.

the dependence of $V_{el}$ on the intermolecular distance which is obtained from the atomic increment method (section 4). The experimental results in *N*-monoalkylanilines rather suggest that the intermolecular distance is independent of the size of the alkyl group. We will discuss the reason in the following section.

**6.4. Deuterium Isotope Effect on the Electron-Transfer Dynamics: *N*-Monoalkylanilines.** Table 1 lists the results on the ET dynamics using *N*-deuterated *N*-monoalkylanilines as the electron donating solvents. There are two noticeable points in the table, and the first one is that there is almost no deuterium isotope effect on the ET dynamics for C151, a fast ET system, but a large isotope effect is clearly seen for C153 (∼20%), a slow ET system. These results are very similar to our previous results[32] on deuterated aniline as the donor solvent, where the origin of the isotope effect was explained in terms of the intermolecular hydrogen-bonding interaction in the liquid. Similarly, the deuterium isotope effect on the ET in the present cases arises from changes in $\Delta G^0$ by the deuterated solvent donors. The hydrogen-bonding interaction is stabilized more in deuterated solvent than in normal solvent, because the zero-point energy of hydrogen bond in normal solvent is higher than that in deuterated solvent.[75−77] The more stabilized intermolecular hydrogen-bonding interaction should cause a more organized intermolecular structure to reduce the entropy in the system. Thus, for the present systems it is expected that the isotopic substitution of the solvent, *N*-monoalkylaniline, can cause a reduction in the driving force.

As a support for this effect on the driving force of the ET dynamics, the oxidation potentials of the donor molecules become more positive in the deuterated solvents than in the normal solvents (Table 3 and ref 32). Similarly, the reduction potentials of the dyes in the deuterated solvents are more negative than those in the normal solvents (Table 3 and ref 32). These observations thus suggest that $\Delta G^0$ for the ET dynamics is reduced in the deuterated solvent due to the solvent structural effect arising from the intermolecular hydrogen bonds. This is probably the main reason for the observed isotope effect on the ET dynamics in the present system.

Since the ET of C151 corresponds to the barrierless region of the $k_{ET}$ vs $\Delta G^0$ relation, a small change in $\Delta G^0$ does not give any large effect on the ET rate constant. For C153, however, $\Delta G^0$ is in the normal region where the $k_{ET}$ vs $\Delta G^0$ curve is steep. Thus, a small change in $\Delta G^0$, as caused by the isotopic substitution, yields an appreciable change in the ET

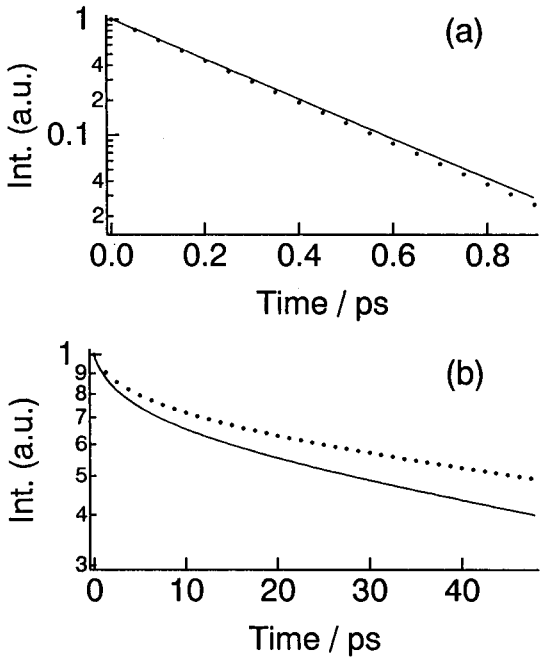


**Figure 14.** Simulated decay curves of C151 (a) and C153 (b) in MAN, (solid line) and MAN-*d*, (dotted line). In fast electron transfer the deuterium isotope effect is very small, but that in slow electron transfer is large. The results between experiment (Figure 6) and simulation are identical.

dynamics. To investigate the origin of the deuterium isotope effect of *N*-monoalkylanilines quantitatively, we simulate the ET rates following the 2D-ET model. We assume that the effect on the ET dynamics is only due to $\Delta G^0$. For the simulation of the ET dynamics in MAN-*d* we use $\Delta G^0$ about 0.02 eV less than that in MAN. That is because the oxidation potentials of donor molecules in the deuterated solvents are about 10 mV more positive than those in the normal solvents, and the reduction potentials of the dyes in the deuterated solvents are also about 10 mV more negative than those in the normal solvents. The free energy gaps with C151 are chosen to be $\Delta G^0 = -0.50$ eV for MAN and $-0.48$ eV for MAN-*d*, and those with C153 are chosen to be $\Delta G^0 = -0.00$ eV for MAN and $+0.02$ eV for MAN-*d*. The solvation parameters used are experimentally obtained values for MAN and MAN-*d* (Table 2). The other ET parameters are assumed to be unchanged by the deuterium substitution.[32] The results of the simulation are shown in Figure 14. Figure 14a shows results for C151 and (b) for C153, where the solid lines are for MAN and dots for MAN-*d* as donors. This figure indicates that the fast ET dynamics (C151) is not much affected by the isotopic substitution, but the slow ET dynamics (C153) is affected substantially (C151 = ∼0% and C153 = ∼20% slower in deuterated analog). This is exactly the same tendency as we observe in the present experiment.

Moreover, the simulation predicts an interesting point, that is, the deuterium isotope effect on the ET dynamics may show the reverse tendency in the inverted region: A rate constant in the deuterated solvents would be faster than that in the normal solvents, because the more negative free energy gap gives slower ET in the inverted region. Figure 15 shows a simulation of the deuterium isotope effect in the inverted region. For the simulation, we choose the $\Delta G^0 = -1.10$ eV for MAN and $\Delta G^0 = -1.08$ eV for MAN-*d*. The other parameters are the same as the previous case. It is clear from Figure 15 that the ET dynamics in the deuterated solvent would be faster than that in the normal solvent if the ET process is in the inverted region.

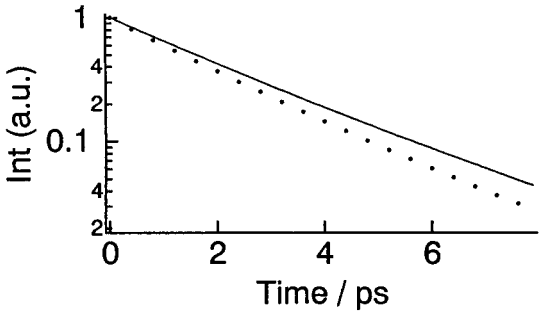


**Figure 15.** Simulated decay curves in the inverted region. All the electron transfer parameters are used for *N*-methylaniline (MAN). Solid line is normal solvent ($\Delta G^0 = -1.10$ eV) and dot line is deuterated solvent ($\Delta G^0 = -1.08$ eV).

However, we do not observe this phenomenon in the present experiments, probably because the present systems are in the normal region.

The second interesting point is that the extent of the deuterium isotope effect on the ET dynamics for a particular coumarin dye is almost similar for all the *N*-monoalkylanilines. These experimental results suggest that the alkyl group does not have much effect on the intermolecular hydrogen bonding in these solvents. Generally, it is explained that the intermolecular hydrogen bonding is formed by the participation of the N−H hydrogen of one molecule and the lone pair electrons on the nitrogen atom of another molecule of the solvent. The microscopic picture for the intermolecular configuration may be following; although a bulky alkyl group is attached on the nitrogen atom of the *N*-monoalkylaniline, there is a space on the N−H group side, which facilitates access of the other molecules such as coumarins or solvents to this N−H group, regardless the size of the alkyl group. Therefore, *the distance between the N-monoalkylaniline and coumarin or the interaction of the hydrogen bond are rather insensitive to the dimension of the alkyl group.*

## 7. Conclusion

We have investigated the substituent effect and deuterium isotope effect of the intermolecular electron transfer (ET) for the system of 7-amino coumarins in electron donor solvents, aniline (AN), *N*-monoalkylanilines, *N*,*N*-dialkylanilines. Differences are evident in the rate of ET ($k_{ET}$) vs free energy gap ($\Delta G^0$) in AN, *N*-methylaniline (MAN), and *N*,*N*-dimethylaniline (DMA). We simulated rate constants based on the 2D-ET model which includes solvent and nuclear coordinates separately. It is suggested that the barrierless ET rates in AN, MAN, and DMA are quite different. This is mainly due to the different electronic matrix elements ($V_{el}$) arising from the different distance-independent electronic matrix elements ($V_{el0}$) of AN, MAN, and DMA.

A larger substituent effect on the ET dynamics is observed among *N*,*N*-dialkylanilines than *N*-monoalkylanilines. It seems that the substituent effect of *N*,*N*-dialkylanilines mainly arises from the effect on the electronic matrix element resulting from the increased distance of the donor−acceptor separation as the bulkier alkyl groups are substituted. In *N*-monoalkylanilines, however, the N−H hydrogen of the amino group keeps enough space on the amino nitrogen of the donor molecules, therefore the ET dynamics is insensitive to the size of one N-alkyl group.

From the deuterium isotope effect of *N*-monoalkylanilines on the ET dynamics, we have confirmed the generality of the isotope effect. The slow coumarin dyes (C152, C481, C522, and C153) show the smaller ET rate by deuterium substitutions of the N−H group of the donor solvents, but the fast coumarin dye (C151) does not show any isotope effect. From the cyclic voltammetric measurement and simulations, it appears that the isotope effect is actually arising from the difference in the stabilization energies of hydrogen-bonding interactions of the deuterated and normal solvents, and this eventually affects $\Delta G^0$. The experimental results show that the deuterium isotope effects on the ET rate for a specific coumarin dye is the same for every *N*-monoalkylanilines. The results of the deuterium isotope effect of *N*-monoalkylanilines are in accordance with the results of the substituent effect of *N*-monoalkylanilines on the ET dynamics. The simulation also indicates that the deuterium isotope effect on ET dynamics in the inverted region should be opposite to that in the normal region.

**Acknowledgment.** We thank Mr. T. Yamanaka and Dr. M. Tomura of IMS for their kind help in all respects. H. Pal gratefully acknowledges Japan Society for the Promotion of Science for the postdoctoral fellowship. This work was partly supported by a Grant-in-Aid for Scientific Research on New Program (Grant 07NP0301) by the Ministry of Education, Science, Sports, and Culture of Japan.

## References and Notes

(1) Marcus, R. M. *Annu. Rev. Phys. Chem.* **1964**, *15*, 155.
(2) Marcus, R. M.; Sutin, N. *Biochim. Biophys. Acta.* **1985**, *811*, 265.
(3) Guarr, T.; McLendon, G. *Coord. Chem. Rev.* **1985**, *68*, 1.
(4) Kosower, E. M.; Huppert, D. *Annu. Rev. Phys. Chem.* **1986**, *37*, 127.
(5) Kavarnos, G. J.; Turro, N. J. *Chem. Rev.* **1986**, *86*, 401.
(6) Closs, G. L.; Miller, J. R. *Science* **1988**, *240*, 440.
(7) Maroncelli, M.; MacInnis, J.; Fleming, G. R. *Science* **1989**, *243*, 1674.
(8) Bagchi, B. *Annu. Rev. Phys. Chem.* **1989**, *40*, 115.
(9) Barbara, P. F.; Jarzeba, W. *Adv. Photochem.* **1990**, *15*, 1.
(10) Weaver, M. J.; McManis III, G. E. *Acc. Chem. Res.* **1990**, *23*, 294.
(11) Barbara, P. F.; Walker, G. C.; Smith, T. P. *Science* **1992**, *256*, 975.
(12) Weaver, M. J. *Chem. Rev.* **1992**, *92*, 463.
(13) Heitele, H. *Angew. Chem., Int. Ed. Engl.* **1993**, *32*, 359.
(14) Yoshihara, K.; Tominaga, K.; Nagasawa, Y. *Bull. Chem. Soc. Jpn.* **1995**, *68*, 696.
(15) Barbara, P. F.; Meyer, T. J.; Ratner, M. A. *J. Phys. Chem.* **1996**, *100*, 13148.
(16) Fox, M. A., Chanon, M., Eds. *Photoinduced Electron Transfer*; Elsevier: Amsterdam, 1988.
(17) Dewar, M. J. S., Dunitz, J. D., Hafner, K., Ito, S., Lehn, J.-M., Niedenzu, K., Raymond, K. N., Rees, C. W., Vögtle, F., Eds. *Topics in Current Chemistry: Photoinduced Electron Transfer*; Springer-Verlag: Berlin Heidelberg, 1993.
(18) Marcus, R. A. *J. Chem. Phys.* **1956**, *24*, 976.
(19) Marcus, R. A. *Discuss. Faraday Soc.* **1960**, *29*, 21.
(20) Zusman, L. D. *Chem. Phys.* **1980**, *49*, 295.
(21) Onuchic, J. N. *J. Chem. Phys.* **1987**, *86*, 3925.
(22) Rips, I.; Jortner, J. *J. Chem. Phys.* **1987**, *87*, 2090.
(23) Calef, D. F.; Wolynes, P. G. *J. Phys. Chem.* **1983**, *87*, 3387.
(24) Kobayashi, T. Takagi, Y.; Kandori, H. Kemnitz, K.; Yoshihara, K. *Chem. Phys. Lett.* **1991**, *180*, 416.
(25) Kandori, H.; Kemnitz, K.; Yoshihara, K. *J. Phys. Chem.* **1992**, *96*, 8042.
(26) Yartsev, A.; Nagasawa, Y.; Douhal, A.; Yoshihara, K. *Chem. Phys. Lett.* **1993**, *207*, 546.
(27) Nagasawa, Y.; Yartsev, A. P.; Tominaga, K.; Johnson, A. E.; Yoshihara, K. *J. Am. Chem. Soc.* **1993**, *115*, 7922.
(28) Yoshihara, K.; Yartsev, A.; Nagasawa, Y.; Kandori, H.; Douhal, A.; Kemnitz, K. *Pure Appl. Chem.* **1993**, *65*, 1671.
(29) Yoshihara, K.; Nagasawa, Y.; Yartsev, A.; Kumazaki, S. Kandori, H.; Johnson, A. E.; Tominaga, K. *J. Photochem. Photobiol., A* **1994**, *80*, 169.
(30) Nagasawa, Y.; Yartsev, A. P.; Tominaga, K.; Johnson, A. E.; Yoshihara, K. *J. Chem. Phys.* **1994**, *101*, 5717.
(31) Nagasawa, Y.; Yartsev, A. P.; Tominaga, K.; Bisht, P. B.; Johnson, A. K.; Yoshihara, K. *J. Phys. Chem.* **1995**, *99*, 653.
(32) Pal, H.; Nagasawa, Y.; Tominaga, K.; Yoshihara, K. *J. Phys. Chem.* **1996**, *100*, 11964.
(33) Sumi, H.; Marcus, R. A. *J. Chem Phys.* **1986**, *84*, 4894.
(34) Agmon, N.; Hopfield, J. J. *J. Chem. Phys.* **1983**, *78*, 6947.

(35) Bagchi, B.; Fleming, G. R.; Oxtoby, D. W. *J. Chem. Phys.* **1983**, *78*, 7375.
(36) Bixon, M.; Jortner, J. *Chem. Phys.* **1993**, *176*, 467.
(37) Johnson, A. E.; Levinger, N. E.; Jarzeba, W.; Sclief, R. E.; Kleiner, D. A.; Barbara, P. F. *Chem. Phys.* **1993**, *176*, 555
(38) Kleiner, D. A. V.; Tominaga, K.; Walker, G. C.; Barbara, P. F. *J. Am. Chem. Soc.* **1992**, *114*, 8323.
(39) Tominaga, K. Kleiner, D. A. V.; Johnson, A. E. Levinger, N. E.; Barbara, P. F. *J. Chem. Phys.* **1993**, *98*, 1228.
(40) Jones, II, G.; Jackson, W. R.; Halpern, A. M. *Chem. Phys, Lett.* **1980**, *72*, 391.
(41) Jones, II, G.; Jackson, W. R.; Choi, C.; Bergmark, W. R. *J. Phys. Chem.* **1985**, *89*, 294.
(42) Rechthaler, K.; Kohler, G. *Chem. Phys.* **1994**, *189*, 99.
(43) Maroncelli, M. *J. Mol. Liq.* **1993**, *57*, 1.
(44) Rosenthal, S. J.; Jimenetz, R.; Fleming, G. R.; Kumer, P. V.; Maroncelli, M. *J. Mol. Liq.* **1994**, *60*, 25.
(45) Nagarajan, V.; Brearley, A. M.; Kang, T. J.; Barbara, P. F. *J. Chem. Phys.* **1987**, *86*, 3138.
(46) Kahlow, M. A. Kang, T. J.; Barbara, P. F. *J. Chem. Phys.* **1988**, *88*, 2372.
(47) Pal, H.; Nagasawa, Y.; Tominaga, K.; Kumazaki, S.; Yoshihara, K. *J. Chem. Phys.* **1995**, *102*, 7758.
(48) Shirota, H.; Pal, H.; Tominaga, K.; Yoshihara, K. *J. Phys. Chem.* **1996**, *100*, 14575.
(49) Horng, M. L.; Gardecki, J. A.; Papazyan, A.; Maroncelli, M. *J. Phys. Chem.* **1995**, *99*, 17311.
(50) Reynolds, L.; Gardecki, J. A.; Frankland, S. J. V.; Horng, M. L.; Maroncelli, M. *J. Phys. Chem.* **1996**, *100*, 10337.
(51) Smith, N. A.; Lin, S.; Meech, S. R.; Yoshihara, K. *J. Phys. Chem. A* **1997**, *101*, 3641.
(52) Smith, N. A.; Lin, S.; Meech, S. R.; Shirota, H.; Yoshihara, K. *J. Phys. Chem. A* **1997**, *101*, 9578.
(53) Tominaga, K.; Walker, G. C.; Jarzeba, W.; Barbara, P. F. *J. Phys. Chem.* **1991**, *95*, 10475.
(54) Rehm. D.; Weller, A. *Isr. J. Chem.* **1970**, *8*, 259.
(55) Weller, A. *Z. Phys. Chem. N. F.* **1982**, *133*, 93.
(56) Oevering, H.; Paddon-Raw, M. N.; Heppener, M.; Oliver, A. M.; Cotsaris, E.; Verhoeven, J. W.; Hush, N. S. *J. Am. Chem. Soc.* **1987**, *109*, 3258.
(57) Gaines, III, G. L.; O'Neil, M. P.; Svec, W. A.; Niemczyk, M. P.; Wasielewski, M. R. *J. Am. Chem. Soc.* **1991**, *113*, 719.
(58) Fawcett, W. R. *J. Phys. Chem.* **1993**, *97*, 9540.
(59) Fawcett, W. R. *Quantitative Treatments of Solute/Solvent Interactions*; Elsevier: Amsterdam, 1994; p 183.
(60) Edward, J. T. *J. Chem. Educ.* **1970**, *47*, 261.
(61) Dimroth, K.; Reichardt, C.; Siepmann, T.; Bohlmann, F. *Liebigs Ann. Chem.* **1966**, *661*, 1.
(62) Gutmann, V.; Wychera, E. *Inorg. Nucl. Chem. Lett.* **1966**, *2*, 257.
(63) Marcus, Y. *J. Solution Chem.* **1991**, *20*, 929.
(64) Marcus, Y. *J. Solution Chem.* **1984**, *13*, 599.
(65) *CRC Handbook of Chemistry and Physics* 59th ed.; CRC Press: West Palm Beach, 1978.
(66) Walker, G. C.; Akesson, E.; Johnson, A. E.; Levinger, N. E.; Barbara, P. F. *J. Phys. Chem.* **1992**, *96*, 3728.
(67) Jortner, J.; Bixon, M. *J. Chem. Phys.* **1988**, *87*, 167.
(68) Hynes, J. T. *J. Phys. Chem.* **1986**, *90*, 3701.
(69) Kang, T. J.; Jarzeba, W.; Barbara, P. F.; Fonseca, T. *Chem. Phys.* **1990**, *149*, 81.
(70) Matsuda, Y.; Shono, A.; Iwakura, C.; Ohshiro, Y.; Agawa, T.; Tamura, H. *Bull. Chem. Soc. Jpn.* **1971**, *44*, 2960.
(71) Tripathi, G. N. R.; Schuler, R. H. *Chem. Phys. Lett.* **1984**, *110*, 542.
(72) Tripathi, G. N. R.; Schuler, R. H. *J. Chem. Phys.* **1987**, *86*, 3795.
(73) Poizat, O.; Guichard, V.; Buntinx, G. *J. Chem. Phys.* **1989**, *90*, 4697.
(74) Nagasawa, Y. Thesis (The Graduate University for Advanced Studies) 1994. The fluorescence decays of C151 in AN and DMA were measured at 405, 395, and 385 nm. Although the energy difference between 405 and 385 nm lights is as large as 0.16 eV, the decays matched exactly within the experimental error.
(75) Némethy, G.; Scheraga, H. A. *J. Chem. Phys.* **1964**, *41*, 680.
(76) Frank, H. S. *Water*; Plenum: New York, 1972; Vol.1, Chapter 14.
(77) Bürgi, T.; Droz, T.; Leutwyler, S. *Chem. Phys. Lett.* **1995**, *246*, 291.